

# Tandem Cofacial Stacks of Porphyrin–Phthalocyanine Dyads through Complementary Coordination

Mitsuhiko Morisue<sup>[a, c]</sup> and Yoshiaki Kobuke<sup>\*[a, b]</sup>

**Abstract:** A novel straightforward methodology to organize discrete heterogeneous stacks of porphyrin and phthalocyanine employed an imidazolyl-to-zinc complementary coordination protocol for a Zn<sup>II</sup> phthalocyanine that contains an imidazolyl terminal with an ethynylporphyrin as a coplanar spacer. Structural elucidation was performed by means of size-exclusion chromatography, spectral titration, and NMR spectroscopy. The association constants for the complementary coordination of the heterogeneous slipped-cofacial tetrads reached extremely high values, in

the order of 10<sup>14</sup> M<sup>-1</sup>. Close contact of the porphyrin and phthalocyanine planes led to a strong shielding of the cofacial protons, which were split due to the slipped-cofacial heterogeneous environment. In variable-temperature NMR spectroscopy, the split signals remained in the aromatic region, a result suggesting structural robustness. Addition of trifluoroacetic acid dissociated

the coordination structure to unify the split signals. The stacked tetrads showed unique electronic structures, such as strong exciton coupling and charge-transfer properties between the porphyrin and phthalocyanine units, which were modulated by the peripheral substituents of the phthalocyanine subunit and by the solvent. Interconversion between the coordination tetrad and the corresponding dyad was observed upon addition of an axial ligand.

**Keywords:** charge transfer • coordination • molecular organization • phthalocyanines • porphyrinoids

## Introduction

Mutual interplays of sophisticated chromophore stacks play crucial roles in photophysical processes, such as exciton coupling,<sup>[1]</sup> charge-resonance (intervalence) properties,<sup>[2,3]</sup> charge-transfer (CT) interactions,<sup>[3–5]</sup> and nonlinear optical

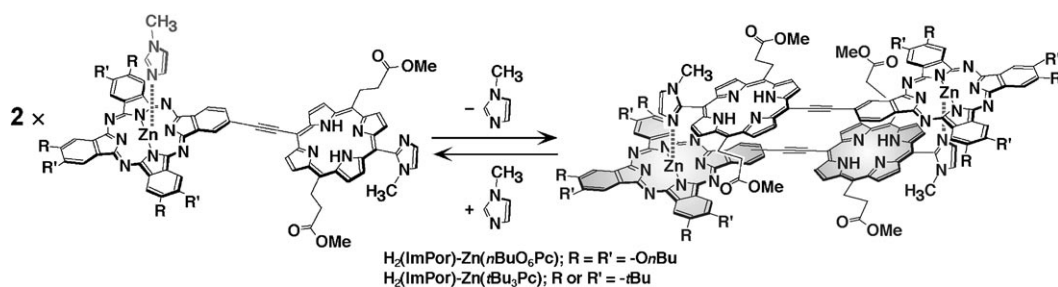
characteristics.<sup>[6]</sup> Of particular interest, pivotal functions of natural photosynthesis are operated by spatially arranged slipped-cofacial stacks of chlorophyll pigments in a “special pair” at the reaction center and in light-harvesting antenna complexes of purple bacteria.<sup>[7]</sup> Mimetically, an imidazolyl substitution at the *meso* position of zinc porphyrin or the  $\beta$  position of zinc phthalocyanine (Zn(ImPor) or Zn(ImPc),<sup>[8,9]</sup> respectively) can organize the corresponding dimer into a slipped-cofacial configuration by imidazolyl-to-zinc complementary coordination. The slipped-cofacial dimers are formed with extremely large stability constants (10<sup>11</sup>–10<sup>12</sup> M<sup>-1</sup>) in noncoordinating solvents.<sup>[8,9]</sup> The Zn(ImPor) unit can thus provide a powerful tool for further tailoring successive arrays in linear and cyclic arrangements.<sup>[10]</sup> Furthermore, the Zn(ImPor) cofacial dimer serves as a good charge-separation unit,<sup>[11]</sup> as a photosensitizer for photocurrent generation,<sup>[12]</sup> and in nonlinear optical materials.<sup>[13]</sup> A cofacially stacked configuration enhances electronic communication through proximal  $\pi$ -electron contact between donor and acceptor aromatic systems; this may be used for the aim of fabricating a novel  $\pi$ -electron system.<sup>[3–5]</sup> Employing the complementary coordination protocol, we herein report a novel straightforward approach to organize cofacial donor–acceptor stacks.

[a] Dr. M. Morisue, Prof. Dr. Y. Kobuke  
Graduate School of Materials Science  
Nara Institute of Science and Technology  
Ikoma 630–0192 (Japan)  
E-mail: kobuke@iae.kyoto-u.ac.jp

[b] Prof. Dr. Y. Kobuke  
Current address: Institute of Advanced Energy  
Kyoto University, Gokasho, Uji  
Kyoto 611–0011 (Japan)

[c] Dr. M. Morisue  
Current address: Department of Biomolecular Engineering  
Kyoto Institute of Technology, Matsugasaki, Sakyo-ku  
Kyoto 606–8585 (Japan)

Supporting information for this article is available on the WWW under <http://www.chemeurj.org/> or from the author. It contains <sup>1</sup>H, <sup>13</sup>C, COSY, ROESY, HMQC, and HMBC NMR spectra and competitive titration results.



Scheme 1. Dyad–tetrad equilibrium of  $H_2(\text{ImPor})\text{-Zn}(\text{Pc})$ .

The combination of a porphyrin–phthalocyanine (Por–Pc) pair as an energy donor–acceptor dyad is intriguing due to the intense absorption by the Soret band of Por in the visible region and by the Q band of Pc in the near-IR region. In addition, the ideal overlap of emission of Por and the Q band of Pc ensures efficient funneling of photoexcitation energy into the Pc subunit.<sup>[14–16]</sup> Previously, we reported efficient energy transfer and succeeding electron-transfer reactions in the directly connected  $\text{Zn}(\text{ImPor})\text{-Zn}(\text{Pc})$  couple, one of the closest covalent systems in the orthogonal configuration, wherein the slipped-cofacial dimer stabilized a radical ion pair to contribute to a prolonged charge-separation state.<sup>[16b]</sup> Alternatively, a stacked electron donor–acceptor pair forming a CT complex is an attractive candidate for producing a charge-separated state<sup>[5]</sup> and potential further elaborate molecular systems.<sup>[17]</sup> Indeed, an intradimer CT system couples the efficient electron-transfer reaction in natural photosynthesis.<sup>[18]</sup> Among these systems, stacked arrays of metallophthalocyanines receive great attention in current research.<sup>[19]</sup> The cofacially stacked configuration with a van der Waals contact should be the closest structure to arrange two donor and acceptor units. The increase in  $\pi$ -electron communication will offer novel photoelectronic applications. When ethynyl-conjugated porphyrin intervenes between the imidazolyl terminal and phthalocyaninatozinc,  $\text{Zn}(\text{Pc})$ , complementary coordination of the imidazolyl group to the central zinc atom of a Pc subunit is envisaged to organize heterogeneous slipped-cofacial stacks of Por and Pc planes based on their coplanar configuration (Scheme 1). Such Por–Pc couples will emerge as a promising class of material for not only one-photon light harvesting but also two-photon absorption.<sup>[13,20–22]</sup>

## Results and Discussion

**Coordination properties:** The basic principle for the organization of the heterogeneous cofacial stacks employs the complementary coordination protocol, which has been established for the slipped-cofacial dimer formation of  $\text{Zn}(\text{ImPor})$  and  $\text{Zn}(\text{ImPc})$ .<sup>[8,9]</sup> First, we examined the coordination properties.

The molecular weight was estimated by means of analytical size-exclusion chromatography (SEC). SEC showed a single peak corresponding to the molecular size of the coordi-

ination tetrad. The retention time, monitored at multiple wavelengths (450, 685, 690, and 750 nm), was compared to that of a polystyrene standard. Each stacked tetrad coincidentally showed a single peak at each monitored wavelength (Figure 1). The  $H_2(\text{ImPor})\text{-Zn}(\text{Pc})$  dyad was proved to exist as the converged species. The molecular weights were estimated as 2100 and 2700 for  $H_2(\text{ImPor})\text{-Zn}(t\text{Bu}_3\text{Pc})$  and  $H_2(\text{ImPor})\text{-Zn}(n\text{BuO}_6\text{Pc})$ , respectively, from the retention times (Figure 1c). These values are smaller than the calculated ones (2656 and 3192 for the tetrads of  $H_2(\text{ImPor})\text{-Zn}(t\text{Bu}_3\text{Pc})$  and  $H_2(\text{ImPor})\text{-Zn}(n\text{BuO}_6\text{Pc})$ , respectively). Such deviations are normally considered to be due to geometrical

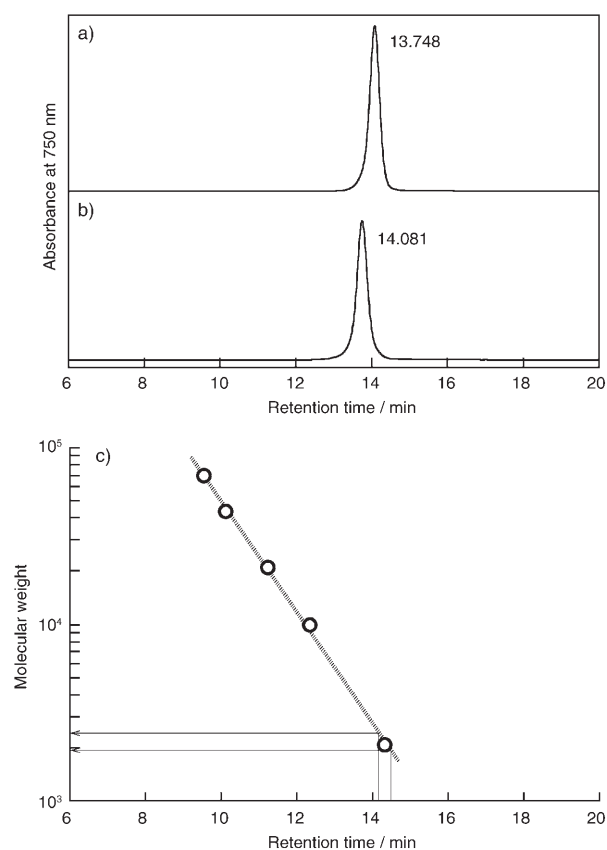


Figure 1. Size-exclusion chromatographic traces of a)  $H_2(\text{ImPor})\text{-Zn}(t\text{Bu}_3\text{Pc})$  and b)  $H_2(\text{ImPor})\text{-Zn}(n\text{BuO}_6\text{Pc})$  eluted with  $\text{CHCl}_3$ , c) Logarithmic plot of molecular weight with reference to polystyrene as a standard.

differences with the polystyrene standard.<sup>[23]</sup> It was thus inferred that the H<sub>2</sub>(ImPor)–Zn(Pc) dyad was converged into the coordination tetrad structure in a noncoordinating solvent. Tetrad formation was also suggested by MALDI-TOF mass spectrometry. A clear peak assignable to the tetrad structure was observed, in addition to the dissociated dyad under the ionization conditions (Figure 2). Details of the assembling properties are described below.

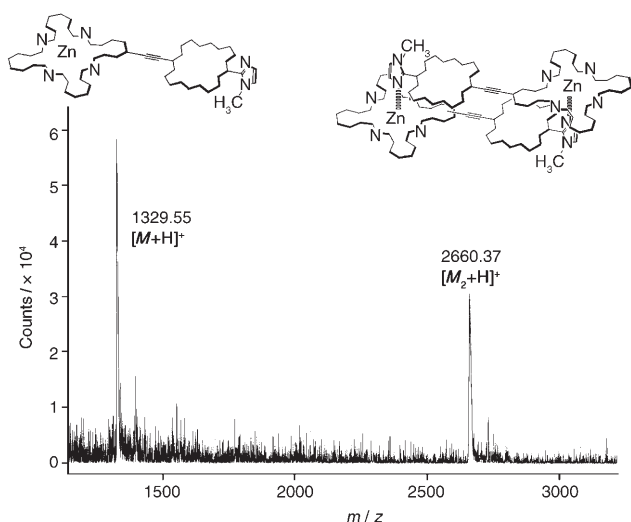
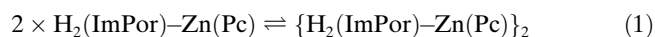


Figure 2. MALDI-TOF mass spectrum of H<sub>2</sub>(ImPor)–Zn(*t*Bu<sub>3</sub>Pc) observed in the positive mode with dithranol as the matrix. The calculated values for the dyad and tetrad are 1328.48 and 2656.96, respectively.

The coordination behaviors of the stacked H<sub>2</sub>(ImPor)–Zn(Pc) tetrads were elucidated by spectral titration. Dissociation of the tetrad upon addition of 1-methylimidazole as a competitive axial ligand was shown as a spectral change through isosbestic points (Figure 3a). The spectral evolution evidenced that the organized structures were directed by imidazolyl-to-zinc complementary coordination.

From this titration, the association constant  $K_1$ , for the equilibrium between the dissociated dyad and the stacked tetrad [Eq. (1)] can be described according to Equation (2).



$$K_1 = [\{\text{H}_2(\text{ImPor})\text{--Zn}(\text{Pc})\}_2] / [\text{H}_2(\text{ImPor})\text{--Zn}(\text{Pc})]^2 \quad (2)$$

The dissociated dyad was not observed without addition of an axial ligand. The association constant  $K_1$  can then be determined by using the association constants  $K_2$  and  $K_3$  [Eq. (3) and (4)].

$$K_2 = [\text{H}_2(\text{ImPor})\text{--Zn}(\text{Pc}) \cdot \text{Im}]^2 / [\{\text{H}_2(\text{ImPor})\text{--Zn}(\text{Pc})\}_2][\text{Im}]^2 \quad (3)$$

$$K_3 = [\text{Zn}(\text{Pc}) \cdot \text{Im}] / [\text{Zn}(\text{Pc})][\text{Im}] \quad (4)$$

The value of  $K_2$  can be experimentally estimated for the

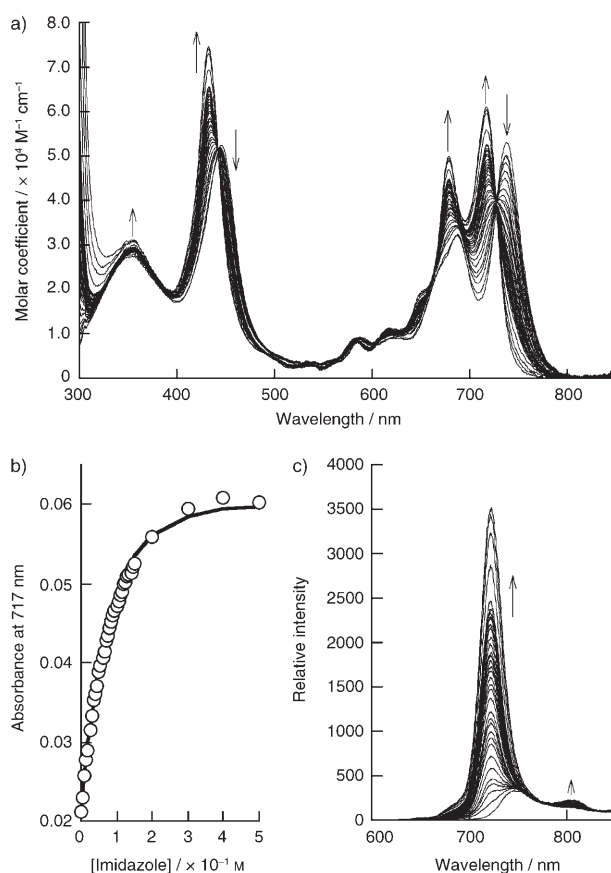
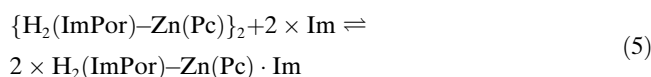


Figure 3. a) Spectral titration of H<sub>2</sub>(ImPor)–Zn(*t*Bu<sub>3</sub>Pc) with 1-methylimidazole in toluene at 25 °C and b) the corresponding titration curve ([H<sub>2</sub>(ImPor)–Zn(*t*Bu<sub>3</sub>Pc)] = 1.0 × 10<sup>−6</sup> M). c) Fluorescence spectra normalized at the excitation wavelength (455 nm).

equilibrium in Equation (5).



Thus, the  $K_2$  values for H<sub>2</sub>(ImPor)–Zn(*t*Bu<sub>3</sub>Pc) and H<sub>2</sub>(ImPor)–Zn(*n*BuO<sub>6</sub>Pc) were determined as 3.1 × 10<sup>−4</sup> and 4.9 × 10<sup>−4</sup> M<sup>−1</sup>, respectively. The binding constant  $K_3$  was previously determined by the Scatchard method for the equilibrium in Equation (6), wherein Zn(Pc) denotes the reference compounds tetrakis(*tert*-butyl)phthalocyaninatozinc, Zn(*t*Bu<sub>4</sub>Pc), or octa(*n*-butoxy)phthalocyaninatozinc, Zn(*n*BuO<sub>8</sub>Pc).



The  $K_3$  values were 3.4 × 10<sup>5</sup> and 2.8 × 10<sup>5</sup> M<sup>−1</sup> for Zn(*t*Bu<sub>4</sub>Pc) and Zn(*n*BuO<sub>8</sub>Pc), respectively.<sup>[9]</sup> Through combination of the  $K_2$  and  $K_3$  values, the desired  $K_1$  value is defined according to Equation (7).

$$K_1 = K_3^2 / K_2 \quad (7)$$

Thus, the self-association constants for  $H_2(\text{ImPor})\text{-Zn}(t\text{Bu}_3\text{Pc})$  and  $H_2(\text{ImPor})\text{-Zn}(n\text{BuO}_6\text{Pc})$  were estimated to be  $3.7 \times 10^{14}$  and  $1.6 \times 10^{14} \text{ M}^{-1}$ , respectively, in toluene. Coordination assisted by a larger  $\pi$ -electron framework and strong CT interactions may have resulted in such high values compared to the value in the order of  $10^{12} \text{ M}^{-1}$  for the directly imidazolyl-substituted  $\text{Zn}(\text{ImPc})$  cofacial dimer.<sup>[9]</sup> Complementary coordination methodology is thus feasible for the organization of discrete cofacial donor–acceptor stacks with extremely large stability constants.

**Cofacially stacked structure:** The detailed coordination structure of  $H_2(\text{ImPor})\text{-Zn}(n\text{BuO}_6\text{Pc})$  was elucidated by NMR spectroscopy in  $\text{CDCl}_3$  (Figure 4). Complementary co-

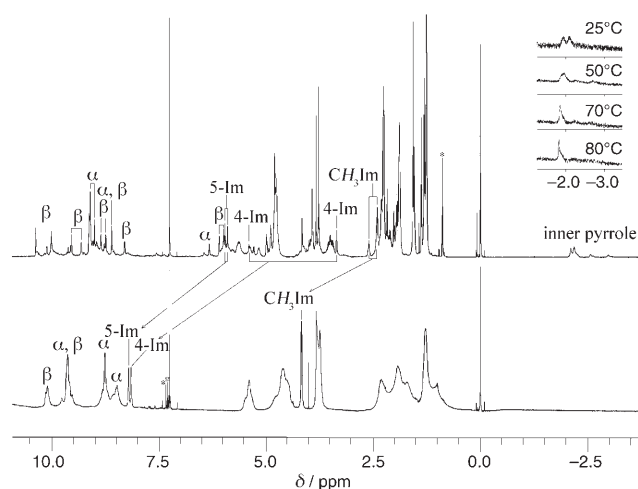


Figure 4.  $^1\text{H}$  NMR spectra of  $H_2(\text{ImPor})\text{-Zn}(n\text{BuO}_6\text{Pc})$  in  $\text{CDCl}_3$  at room temperature (600 MHz). The stacked tetrad (upper spectrum) was dissociated by addition of 10% trifluoroacetic acid (TFA; lower spectrum). “ $\alpha$ ”, “ $\beta$ ”, and “\*” denote the protons in the  $\alpha$  position of the Pc ring, of the  $\beta$ -pyrrole group of the Por subunit, and in an impurity, respectively. The inset shows the temperature dependence of the inner NH protons in  $[\text{D}_8]\text{toluene}$  with an aliquot of  $\text{CDCl}_3$ .

ordination should place the cofacial Por and Pc planes in the proximal positions. The interplanar distance of stacked Por and Pc planes is assumed to be as close as  $3.23 \text{ \AA}$ , as determined by X-ray crystallography for the cofacial dimer of  $\text{Zn}(\text{ImPor})$ .<sup>[8c]</sup> Strong shielding by the cofacial Por or Pc plane should then result in the upfield shift of the corresponding signals.

Structural dissymmetry arising from substitution at the  $\beta$  position of the Pc ring provides two possible structural isomers for the coordination tetrad, represented as “parallel” and “oblique” geometries (Figure 5). The existence of a regioisomer due to the structural dissymmetry was elucidated previously in the slipped-cofacial dimer of  $\beta$ -imidazolyl  $\text{Zn}(\text{Pc})$ ,  $\text{Zn}(\text{ImPc})$ .<sup>[9]</sup> In a similar manner, the  $\beta$ -imidazolyl  $\text{Zn}(\text{Pc})$  intervened with ethynylporphyrin,  $H_2(\text{ImPor})\text{-Zn}(\text{Pc})$ , should form complementary coordination with two geometrical isomers. All the protons, therefore, should show duplicate signals. Moreover, dissymmetric orientation dis-

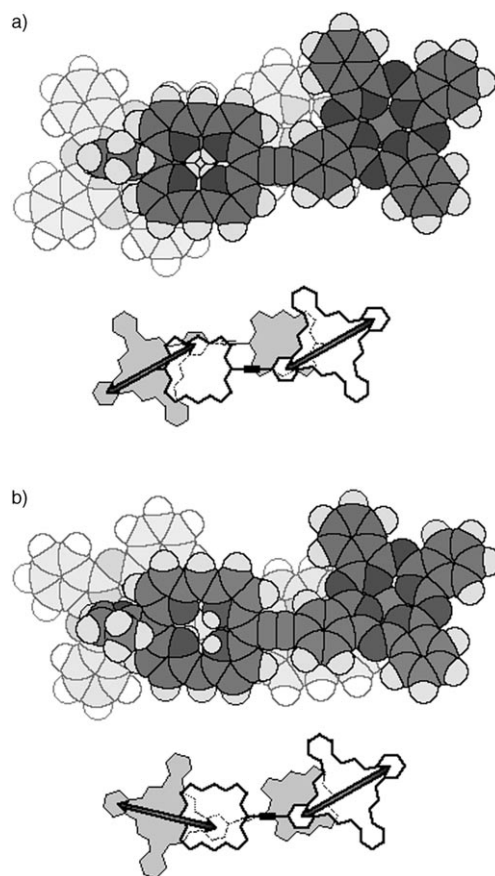


Figure 5. Parallel and oblique geometric isomers of the stacked tetrad. The molecular structures were drawn by the AM1 method with the WinMOPAC V.3.9 software (Fujitsu), with the aliphatic side chains omitted for visual clarity. The arrows represent the transition dipoles along the long axis of  $\text{Zn}(\text{Pc})$  arranged in a) parallel and b) oblique configurations.

rupts the structural symmetry of the Por and Pc planes to distribute all of the protons into individual signals in each regioisomer. Therefore, in principle, all of the  $\alpha$  protons of the Pc plane and the  $\beta$ -pyrrole group of the Por plane should show individual peaks (16 peaks for one regioisomer; therefore, a total of 32 peaks) due to the heterogeneous shielding. The signals were partially assigned by COSY, ROESY, HMQC, and HMBC NMR spectral observations (see the Supporting Information), although complete assignment was difficult because there were too many signals.

The peaks of the  $\beta$ -pyrrole and imidazolyl residues on the  $H_2(\text{ImPor})$  subunit showed upfield shifts, thereby indicating a location close to the Pc plane. In the same manner, shielding by the Por plane leads to upfield shifts and splitting of the signals for the  $\alpha$  protons of the  $\text{Zn}(\text{Pc})$  subunit. These protons showed no significant change upon elevation of the temperature in  $[\text{D}_8]\text{toluene}$  (data not shown). Temperature independence of the NMR spectra suggests that the coordination tetrad is stable, as observed by spectral titration.

The protons of the imidazolyl residue showed simple duplication arising from the structural geometries. The characteristic signals of the imidazolyl residue are most suitable

for evaluation of the stacked structure. Addition of TFA protonated the imidazolyl residue and dissociated the coordination tetrad into the dyad. The duplicated signals converged to unified peaks in the downfield area (Figure 4, bottom), since the structural diversity due to regioisomer formation did not exist in the dissociated dyad. Coincidentally, the split signals of the  $\alpha$  protons of the Pc plane and the  $\beta$ -pyrrole group of the Por plane were simplified by dissociation. Such NMR spectroscopic behavior proved the stacked structure of the Por and Pc planes, in the same manner as in the case of the Zn(ImPc) dimer.<sup>[9]</sup>

Splitting of the signals for the inner NH protons suggests that the heterogeneous environment discriminated two possible tautomers for the diagonal NH protons of the Por subunit. Free-base porphyrin is in equilibrium between two tautomers, which are not discriminated under normal conditions. The inner NH protons of free-base porphyrin are not equivalent due to the dissymmetric geometry in the vicinity of the phthalocyanine plane (Figure 5). Therefore, the dissymmetric environment in the coordination tetrad may discriminate the NH protons of the tautomers. Actually, upon elevation of the temperature in  $[D_8]$ toluene, the multiplet signals of the NH protons coalesced at around 50 °C and then converged to the asymmetric relatively sharp signal, which probably represents the two species attributed to the regioisomers (Figure 4, inset), even though the signals of the aromatic protons were not affected by temperature variation. The downfield shift of the NH protons at higher temperature will stem from the effect of water contained in the system. The dissymmetric broad peak at 80 °C may involve two broad peaks attributed to the regioisomers. This is coincident with no significant shift of the aromatic proton signals. It is assumed that the peaks of the inner NH protons of the porphyrin subunit are the sum of eight signals. Heterogeneous stacking significantly disrupted the structural symmetry of the porphyrin and phthalocyanine planes, which was relevant to the spectral properties of the electronic structures (see below). <sup>1</sup>H NMR spectroscopy elucidates the tautomerism of the inner NH protons and robustness of the coordination-stacked tetrad structure.

**Unique electronic structures:** The slipped-cofacial stack of Por and Pc planes should ensure strong  $\pi$ -electron overlap. The stacked  $H_2(\text{ImPor})\text{-Zn}(\text{tBu}_3\text{Pc})$  tetrad showed large bathochromic shifts for both the Q band of the Pc ring and the Soret band of the Por ring (Figure 3a). In addition, tetrad formation restricts the free rotation around the ethynyl bond to enhance the electronic communication between the coplanar Por and Pc subunits. The bathochromic shift may be interpreted in terms of Kasha's molecular exciton theory for the extended  $\pi$  conjugation through the ethynyl linkage and closely faced Por and Pc planes (Figure 6a).<sup>[1,20b]</sup> Strong  $\pi$  conjugation through the ethynyl linkage disrupted degeneration of the Q band of the Zn(Pc) subunit. The longer absorption maximum of the Q band is assignable to the transition dipole along the long axis of the Zn(Pc) subunit. The shorter one originates from the dipole orthogonal

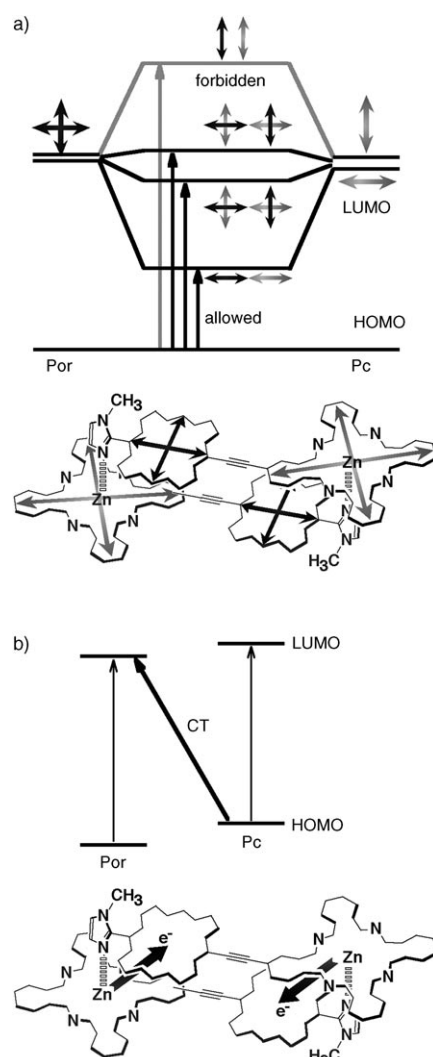


Figure 6. Schematic diagrams of the  $H_2(\text{ImPor})\text{-Zn}(\text{Pc})$  coordination tetrad: a) splitting band levels by exciton coupling, wherein the arrows denote the transition dipoles; b) charge-transfer interactions.

to the above transition dipole of the Zn(Pc) ring. Bathochromism of the coordination tetrad is remarkably larger than that of the orthogonal Zn(ImPor)–Zn(Pc) tetrad, which showed a small broadening of the Q band by cofacial dimer formation of the Zn(ImPor) unit.<sup>[16]</sup> The spectral properties evidenced significant improvement of  $\pi$ -electron communication through the considerable  $\pi$ -electron overlap between the Por and Pc planes.

Besides this, the observed spectral broadening of both the Soret and Q bands may involve CT properties (Figure 6b), since the broadened Q band is reminiscent of the CT properties in Coulombic stacks of Por and Pc.<sup>[24a]</sup> Furthermore, the spectral shape in the Q band region became broader as the dielectric constant of the solvent became larger (Figure 7). Such spectral properties are in line with the general trend in CT properties. Thus, solvent polarity is the predominant factor in modulation of the properties in the absorption spectra.

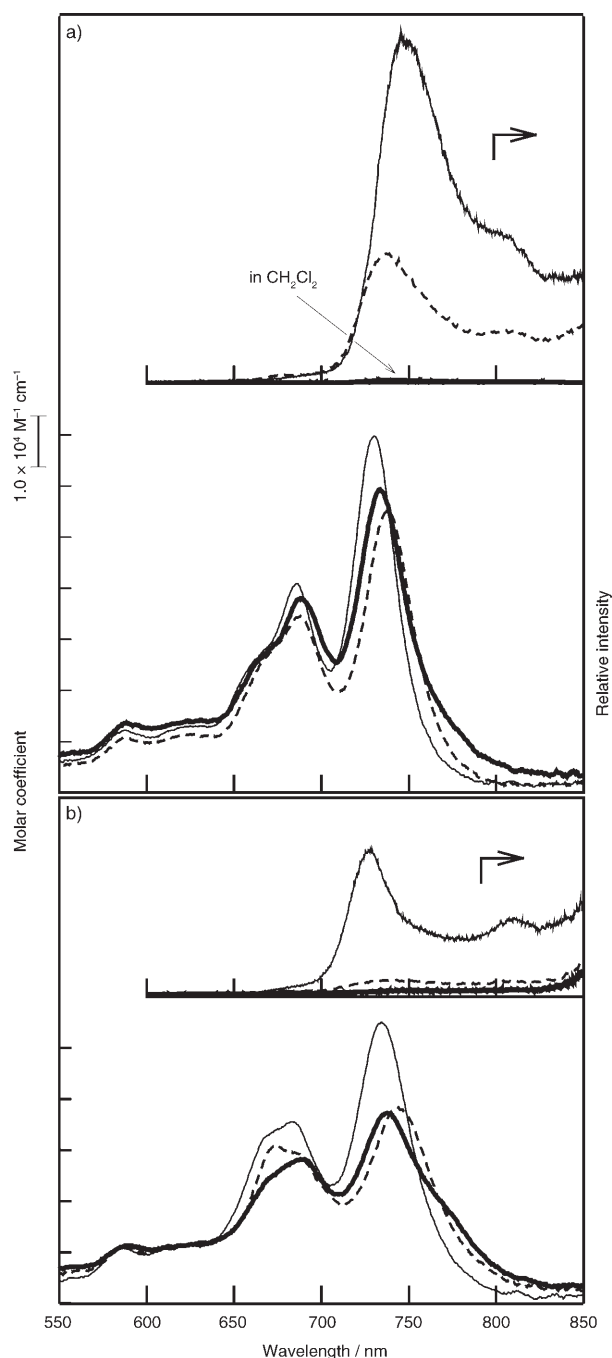


Figure 7. Effect of the solvent and peripheral substituents of the coordination tetrad for a)  $\text{H}_2(\text{ImPor})\text{-Zn}(t\text{Bu}_3\text{Pc})$  and b)  $\text{H}_2(\text{ImPor})\text{-Zn}(n\text{BuO}_6\text{Pc})$  at 25°C. The insets represent the fluorescence spectra excited at 455 nm. —, ----, and —·— represent results recorded in toluene, THF, and  $\text{CH}_2\text{Cl}_2$ , respectively. Both absorption and fluorescence spectra are represented over the same wavelength range.

Further investigation was made by modulating the Pc donor ability through periphery substitution at the  $\beta$  position of the Pc subunit.<sup>[25]</sup> The stronger electron-donating effect of six *n*-butoxy groups results in a higher degree of CT interaction in the stacked  $\text{H}_2(\text{ImPor})\text{-Zn}(n\text{BuO}_6\text{Pc})$  tetrad, as shown by a broader Q band compared to that of the stacked  $\text{H}_2(\text{ImPor})\text{-Zn}(t\text{Bu}_3\text{Pc})$  tetrad in all solvent sys-

tems (Figure 7 and the Supporting Information). Also, the *n*-butoxy groups slightly enhanced the exciton coupling. The effect of the electron-donating substituents supports the above interpretation for the electronic spectra.

$\text{H}_2(\text{ImPor})\text{-Zn}(\text{Pc})$  fluoresces dominantly in the 700–800 nm region, ascribed to Pc-subunit emission, regardless of the coordinated or dissociated species, even if the Soret band of the Por subunit is excited. The efficient energy transfer from  $\text{H}_2(\text{ImPor})$  to the  $\text{Zn}(\text{Pc})$  subunit is due to the ideal overlap of the emission band of Por and the Q band of Pc. The coordination tetrad exhibited no emission at around 680 nm from the Por subunit (Figure 3c and 7), which suggests extremely fast quenching of the excited singlet state. Instead of emission from the Por subunit, fluorescence from the Pc subunit at around 750 nm was observed for both the coordinated and dissociated species (Figure 3c). In particular, the coordination tetrad showed no emission attributed to the Por subunit, whereas the dissociated dyad showed weak fluorescence at around 680 nm. A large spectral shift pronounced the strong exciton coupling. Photoexcitation at the Soret band may, therefore, have relaxed to the exciton state, that is, the resonant molecular orbital composed of Por and Pc subunits (Figure 6a). This assumption accounts well for the complete quenching of fluorescence of the porphyrin in the coordination tetrad.

Weak fluorescence was observed as a distinct characteristic of the coordination tetrad. The emission intensity was significantly decreased as the solvent polarity increased; it also decreased with the introduction of donating peripheral substituents on the  $\text{Zn}(\text{Pc})$  subunit, coincidentally with a similar trend in the CT characteristics in the absorption spectra (Figure 7). The redox potential of the Zn phthalocyanine is susceptible to solvent polarity; thereby, a significant anodic shift of the redox potential is observed upon an increase in solvent polarity.<sup>[26]</sup> The solvent dependence of the redox potential of  $\text{Zn}(\text{Pc})$  is much larger than that of porphyrin. A polar solvent will, therefore, provide a larger potential gap between the Por and Pc subunits to magnify the CT interaction and to quench the fluorescence from the Pc subunit. Interestingly, the fluorescence maximum of the coordination tetrad was shifted to a shorter wavelength than the corresponding absorption maximum of the longer Q band, except for  $\text{H}_2(\text{ImPor})\text{-Zn}(t\text{Bu}_3\text{Pc})$  in toluene (Figure 7). The substantial fluorescence quenching may indicate that the lowest excited singlet state at the longer Q band of the Pc subunit is deactivated by a CT interaction with the cofacial Por subunit. Moreover, in the solvents that induced significant fluorescence quenching ( $\text{H}_2(\text{ImPor})\text{-Zn}(t\text{Bu}_3\text{Pc})$  in  $\text{CH}_2\text{Cl}_2$  and  $\text{H}_2(\text{ImPor})\text{-Zn}(n\text{BuO}_6\text{Pc})$  in THF and  $\text{CH}_2\text{Cl}_2$ ), the longer Q band was accompanied by a shoulder at around 760–780 nm, which may be assignable to the CT band. Upon addition of 1-methylimidazole as a ligand competing with tetrad formation, the fluorescence intensity gradually increased (Figure 3c). The emission of the dissociated  $\text{H}_2(\text{ImPor})\text{-Zn}(\text{Pc})$  dyads was observed from the longer Q band, which indicates photoenergy funneling from the Por to Pc subunits. Although the precise electronic properties of

the coordination tetrad have not been elucidated at the present stage, the photophysical properties show a sharp contrast between the coordination tetrad and the dissociated dyad.

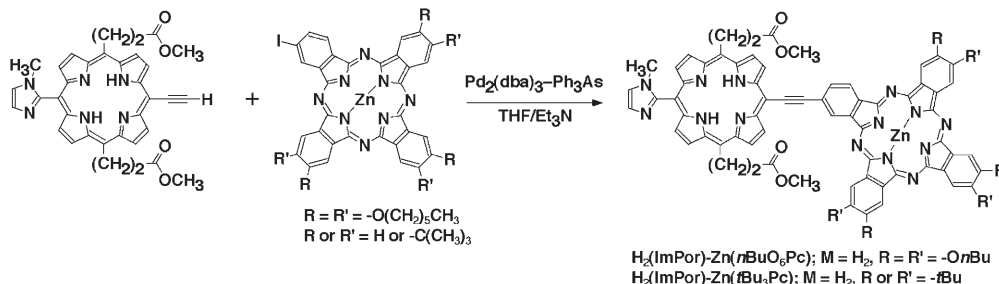
## Conclusion

A complementary coordination protocol has provided a novel straightforward methodology to tailor a discrete donor–acceptor cofacial stack. Heterogeneous stacks of porphyrin and phthalocyanine were organized by self-complementary imidazolyl-to-zinc coordination. The association constants for the coordination tetrads reached  $10^{14} \text{ M}^{-1}$ , which were much higher than those for the coordination homodimers of Zn(ImPor) and Zn(ImPc) ( $10^{11}$ – $10^{12} \text{ M}^{-1}$ ). The self-complementary protocol ensures organization of a discrete donor–acceptor cofacial stack of metalloporphyrinoids with a high stability constant. In the coordination tetrad, interplanar proximity induced significant  $\pi$ -electron interactions between the Por and Pc planes. Tuning of the CT degree between the Por and Pc units is performed by modulation of the donor ability of the Zn(Pc) subunit by the changes in the solvent polarity and peripheral substituents. The CT state in the coordination tetrad was extinguished by addition of an axial ligand to switch to the energy-funneling dyad. The complementary coordination protocol is a promising strategy for organizing discrete donor–acceptor stacks with extremely large association constants.

## Experimental Section

**Synthetic procedures:**  $^1\text{H}$ ,  $^{13}\text{C}$ ,  $^1\text{H}$ – $^1\text{H}$  COSY,  $^1\text{H}$ – $^1\text{H}$  ROESY,  $^1\text{H}$ – $^{13}\text{C}$  HMQC, and  $^1\text{H}$ – $^{13}\text{C}$  HMBC NMR spectra were recorded on a JEOL ECP-600 spectrometer with tetramethylsilane as the internal standard in  $\text{CDCl}_3$ . Temperature variation in  $^1\text{H}$  NMR spectroscopy was carried out in  $[\text{D}_8]$ toluene. MALDI-TOF mass spectrometry was carried out with dithranol as the matrix on a Perseptive Biosystem Voyager DE-STR instrument. THF was distilled over sodium/benzophenone ketyl. Triethylamine ( $\text{Et}_3\text{N}$ ) was distilled over calcium hydride.

**$\text{H}_2(\text{ImPor})\text{--Zn}(\text{nBuO}_6\text{Pc})$ :** Both dyads of  $\text{H}_2(\text{ImPor})\text{--Zn}(\text{Pc})$  were prepared by copper-free Sonogashira coupling (Scheme 2). A mixture of 2-iodo-9,10,16,17,23,24-octa(*n*-butoxy)phthalocyaninatozinc (75 mg,  $66 \times 10^{-6} \text{ mol}$ )<sup>[27]</sup> and 5-ethynyl-10-imidazolylporphyrin (41 mg,  $70 \times 10^{-6} \text{ mol}$ )<sup>[28]</sup> in THF/ $\text{Et}_3\text{N}$  (20/4 mL) was degassed by freeze–pump–thaw cycles and flushed with argon gas in a Schlenk flask. The mixture, with addition of palladium dibenzylideneacetone (16 mg,  $15 \times 10^{-6} \text{ mol}$ ) and



Scheme 2. Synthetic scheme for the dyads. dba: *trans,trans*-dibenzylideneacetone.

triphenylarsine (66 mg,  $64 \times 10^{-6} \text{ mol}$ ) was stirred at  $40^\circ\text{C}$  for 20 h under an argon atmosphere. The reaction mixture was washed with brine and then underwent chromatographic separation. Elution from a silica-gel column (eluent: petroleum ether/chloroform/pyridine 10:30:1) furnished the title compound as a green solid (23 mg,  $15 \times 10^{-6} \text{ mol}$ ; 21%).  $^1\text{H}$  NMR (600 MHz,  $\text{CDCl}_3$ ):  $\delta = -3.15$ – $2.08$  (brm, 2H; inner pyrrole), 1.24–1.38 (m, 18H; Pc  $\text{OCH}_2\text{CH}_2\text{CH}_2\text{CH}_3$ ), 1.87–2.08 (m, 12H; Pc  $\text{OCH}_2\text{CH}_2\text{CH}_2\text{Me}$ ), 2.08–2.30 (m, 12H; Pc  $\text{OCH}_2\text{CH}_2$ ), 2.40, 2.60 (2s, 3H; imidazolyl  $\text{NCH}_3$ ), 3.27, 3.32 (2s, 6H;  $\text{COOCH}_3$ ), 3.35, 5.38 (s, brs, 1H; 4-imidazolyl), 3.36–3.65 (m, 4H; Por  $\text{CH}_2\text{CH}_2\text{COOMe}$ ), 4.19, 4.75, 4.81, 4.84 (3s, t, 12H; Pc  $\text{OCH}_2$ ), 5.62 (brs, 4H; Por  $\text{CH}_2\text{CH}_2\text{COOMe}$ ), 5.92, 5.86 (2s, 1H; 5-imidazolyl), 5.96, 6.08, 8.31, 8.65, 8.77, 8.88, 9.31, 9.58, 10.00, 10.38 (10s, 8H;  $\beta$  positions of the Por ring), 6.31, 8.65, 8.88–9.19 ppm (2s, m, 8H;  $\alpha$  positions of the Pc ring), the  $\beta$  position of the Pc ring was not assignable and may be a broad or multiplet signal;  $^{13}\text{C}$  NMR (150 MHz,  $\text{CDCl}_3$ ):  $\delta = 14.18$ , 14.26, 14.30, 14.34, 14.59, 19.65, 19.70, 19.74, 19.80, 20.05, 22.66, 30.34, 31.59, 31.73, 31.78, 31.91, 32.23, 41.52, 41.73, 51.89, 69.61, 98.10, 102.64, 106.19, 118.95, 119.57, 131.60, 132.16, 132.45, 132.66, 132.81, 132.98, 136.00, 136.57, 145.42, 149.93, 150.75, 151.19, 151.44, 151.60, 151.70, 152.16, 153.54, 153.92, 154.50, 172.96, 173.00, 173.06 ppm; MALDI-TOF MS: *m/z*: calcd: 1592.64; found: 1593.94.

**$\text{H}_2(\text{ImPor})\text{--Zn}(\text{tBu}_3\text{Pc})$ :**  $\text{H}_2(\text{ImPor})\text{--Zn}(\text{tBu}_3\text{Pc})$  was synthesized from 2-iodo-9(10),16(17),23(24)-tri(*tert*-butyl)-phthalocyaninatozinc (four structural isomers, 66 mg,  $76 \times 10^{-6} \text{ mol}$ )<sup>[18a]</sup> 5-ethynyl-10-imidazolylporphyrin (18 mg,  $30 \times 10^{-6} \text{ mol}$ )<sup>[28]</sup> and  $[\text{Pd}_2(\text{dba})_3]$  (6.6 mg,  $6 \times 10^{-6} \text{ mol}$ ), with  $\text{Ph}_3\text{As}$  (23 mg,  $22 \times 10^{-6} \text{ mol}$ ) as the catalyst, in THF/ $\text{Et}_3\text{N}$  (5:2 mL). The coupling conditions and purification procedures were the same as those for the synthesis of  $\text{H}_2(\text{ImPor})\text{--Zn}(\text{nBuO}_6\text{Pc})$ .  $\text{H}_2(\text{ImPor})\text{--Zn}(\text{tBu}_3\text{Pc})$ , as a mixture of four structural isomers, was obtained as a green solid (10 mg,  $7 \times 10^{-6} \text{ mol}$ ; 23%):  $^1\text{H}$  NMR (600 MHz,  $\text{CDCl}_3$ ):  $\delta = -3.06$ – $2.18$  (brm, 2H; inner pyrrole), 1.93–1.98 (m, 27H; *t*Bu), 2.17, 2.19 (2s, 3H; imidazolyl  $\text{NCH}_3$ ), 3.38, 3.44 (2brs, 1H; 4-imidazolyl), 3.58–3.92 (m, 6H;  $\text{COOCH}_3$ ), 3.92–4.32 (brm, 4H; Por  $\text{CH}_2\text{CH}_2\text{COOMe}$ ), 5.04–5.78 (brm, 4H; Por  $\text{CH}_2\text{CH}_2\text{COOMe}$ ), 5.78–6.16, 9.20–9.78 (2brm;  $\alpha$  positions of the Pc ring), 8.00–10.36 ppm (brm;  $\beta$  positions of the Por ring), the peaks for the  $\alpha$  positions of the Pc ring and the  $\beta$  positions of the Por ring were not clearly discriminated, because of complicated signals due to the presence of four structural isomers in the tri(*tert*-butyl)phthalocyanine subunit;  $^{13}\text{C}$  NMR (150 MHz,  $\text{CDCl}_3$ ):  $\delta = 14.125$ , 22.694, 29.364, 29.662, 31.928, 32.264, 32.622, 33.385, 36.102, 36.323, 41.886, 42.245, 51.974, 52.226, 52.302, 71.021, 98.027, 118.84, 119.32, 119.35, 119.50, 122.54, 126.76, 126.99, 127.18, 127.35, 127.49, 128.22, 128.34, 128.42, 128.87, 134.35, 136.85, 139.23, 145.50, 152.93, 153.76, 154.50, 172.90, 173.03, 173.46 ppm; MALDI-TOF MS (see Figure 2): *m/z*: calcd: 1328.48; found: 1329.55.

### Measurements:

**Size-exclusion chromatography:** Analytical size-exclusion chromatograms were recorded by elution with chloroform containing 0.5% ethanol as a stabilizer on a Hewlett–Packard HPI100 series instrument equipped with an analytical JAIGEL 3HA column (Japan Analytical Industry,  $8 \times 500 \text{ mm}$ , exclusion limit: 70000 Da).

**Absorption and fluorescence spectroscopy:** Spectral titration was undertaken at a  $\text{H}_2(\text{ImPor})\text{--Zn}(\text{Pc})$  concentration of  $1.0 \times 10^{-6} \text{ M}$  in each solvent at  $25^\circ\text{C}$ . The absorption spectra were recorded on a Shimadzu UV-

3100PC spectrophotometer. Emission spectra were observed with a Hitachi F-4500 spectrophotometer. Toluene was distilled over sodium. Dichloromethane was dried by distillation over calcium hydride. THF was distilled over sodium/benzophenone ketyl. 1-Methylimidazole was distilled over calcium hydride under reduced pressure.

## Acknowledgements

We gratefully acknowledge the financial support of this work by a Grant-in-Aid for Scientific Research (A) (grant no.: 15205020) from the Ministry of Education, Culture, Sports, Science and Technology, Japan (Monbu Kagakusho).

- [1] M. Kasha, *Radiat. Res.* **1963**, *20*, 55.
- [2] N. Kobayashi, H. Lam, W. A. Nevin, P. Janda, C. C. Leznoff, A. B. P. Lever, *Inorg. Chem.* **1990**, *29*, 3415.
- [3] J. K. Kochi, R. Rathore, P. Le Maguères, *J. Org. Chem.* **2000**, *65*, 6826.
- [4] a) C. A. Hunter, J. K. M. Sanders, *J. Am. Chem. Soc.* **1990**, *112*, 5525; b) C. A. Hunter, K. R. Lawson, J. Perkins, C. J. Urch, *J. Chem. Soc. Perkin Trans. 2*, **2001**, 651; c) E. A. Meyer, R. K. Castellano, F. Diederich, *Angew. Chem.* **2003**, *115*, 1244; *Angew. Chem. Int. Ed.* **2003**, *42*, 1210.
- [5] a) E. Ojad, R. Selzer, H. Linschitz, *J. Am. Chem. Soc.* **1985**, *107*, 7783; b) H. Segawa, C. Takehara, K. Honda, T. Shimidzu, T. Asahi, N. Mataga, *J. Phys. Chem.* **1992**, *96*, 503.
- [6] E. Collini, C. Ferrante, R. Bozio, *J. Phys. Chem. B* **2005**, *109*, 2.
- [7] a) J. Deisenhofer, O. Epp, K. Miki, R. Huber, H. Michel, *Nature* **1985**, *318*, 618; b) G. McDermott, S. M. Prince, A. A. Freer, A. M. Hawthornthwaite-Lawless, M. Z. Papiz, R. J. Cogdell, N. W. Isaacs, *Nature* **1995**, *374*, 517; c) T. Pullerits, V. Sundström, *Acc. Chem. Res.* **1996**, *29*, 381.
- [8] a) Y. Kobuke, H. Miyaji, *J. Am. Chem. Soc.* **1994**, *116*, 4111; b) A. Satake, Y. Kobuke, *Org. Biomol. Chem.* **2007**, *5*, 1679; c) Y. Kobuke, *Struct. Bond.* **2006**, *121*, 49.
- [9] K. Kameyama, M. Morisue, A. Satake, Y. Kobuke, *Angew. Chem.* **2005**, *117*, 4841; *Angew. Chem. Int. Ed.* **2005**, *44*, 4763.
- [10] a) K. Ogawa, Y. Kobuke, *Angew. Chem.* **2000**, *112*, 4236; *Angew. Chem. Int. Ed.* **2000**, *39*, 4070; b) R. Takahashi, Y. Kobuke, *J. Am. Chem. Soc.* **2003**, *125*, 2372.
- [11] H. Ozeki, A. Nomoto, K. Ogawa, Y. Kobuke, M. Murakami, K. Hosoda, M. Ohtani, S. Nakashima, H. Miyasaka, T. Okada, *Chem. Eur. J.* **2004**, *10*, 6393.
- [12] a) M. Morisue, S. Yamatsu, N. Haruta, Y. Kobuke, *Chem. Eur. J.* **2005**, *11*, 5563; b) M. Morisue, D. Kalita, N. Haruta, Y. Kobuke, *Chem. Commun.* **2007**, 2348.
- [13] a) K. Ogawa, A. Ohashi, Y. Kobuke, K. Kamada, K. Ohta, *J. Am. Chem. Soc.* **2003**, *125*, 13356; b) Addition/correction: K. Ogawa, A. Ohashi, Y. Kobuke, K. Kamada, K. Ohta, *J. Am. Chem. Soc.* **2004**, *126*, 4050; c) K. Ogawa, Y. Kobuke, *J. Photochem. Photobiol. C* **2006**, *7*, 1.
- [14] Porphyrin-phthalocyanine dyads: a) S. Gaspard, C. Giannotti, P. Maillard, C. Schaeffer, T.-H. Tran-Thi, *J. Chem. Soc. Chem. Commun.* **1986**, 1239; b) T. H. Tran-Thi, C. Desforge, C. Thiec, S. Gaspard, *J. Phys. Chem.* **1989**, *93*, 1226; c) X.-Y. Li, Q.-F. Zhou, H.-J. Tian, H.-J. Xu, *Chin. J. Chem.* **1998**, *16*, 97; d) H.-J. Tian, Q.-F. Zhou, S.-Y. Shen, H.-J. Xu, *J. Photochem. Photobiol. A* **1993**, *72*, 163; e) M. A. Miller, R. K. Lammi, S. Prathapan, D. Holten, J. S. Lindsey, *J. Org. Chem.* **2000**, *65*, 6634; f) J. M. Sutton, R. W. Boyle, *Chem. Commun.* **2001**, 2014; g) J. P. C. Tomé, A. M. V. M. Pereira, C. M. A. Alonso, M. G. P. M. S. Neves, A. C. Tomé, A. M. S. Silva, J. A. S. Cavaleiro, M. V. Martínez-Díaz, T. Torres, G. M. A. Rahman, J. Ramey, D. M. Guldi, *Eur. J. Org. Chem.* **2006**, 257; h) Y. Bian, X. Chen, D. Wang, C.-F. Choi, Y. Zhou, P. Zhu, D. K. P. Ng, J. Jiang, Y. Weng, X. Li, *Chem. Eur. J.* **2007**, *13*, 4169; i) A. R. M. Soares, M. V. Martínez-Díaz, A. Bruckner, A. M. V. M. Pereira, J. P. C. Tomé, C. M. A. Alonso, M. A. F. Faustino, M. G. P. M. S. Neves, A. C. Tomé, A. M. S. Silva, J. A. S. Cavaleiro, T. Torres, D. M. Guldi, *Org. Lett.* **2007**, *9*, 1557; j) J. Fortage, E. Göransson, E. Blart, H.-C. Becker, L. Hammarström, F. Odobel, *Chem. Commun.* **2007**, 4629, and references cited therein.
- [15] Phthalocyanine-cored multiporphyrins: a) N. Kobayashi, Y. Nishiyama, T. Ohya, M. Sato, *J. Chem. Soc. Chem. Commun.* **1987**, 390; b) N. Kobayashi, T. Ohya, M. Sato, S. Nakajima, *Inorg. Chem.* **1993**, *32*, 1803; c) J. Li, J. R. Diers, J. Seth, S. I. Yang, D. F. Bocian, D. Holten, J. S. Lindsey, *J. Org. Chem.* **1999**, *64*, 9090; d) J. Li, J. S. Lindsey, *J. Org. Chem.* **1999**, *64*, 9101; e) S. I. Yang, J. Li, H. S. Cho, D. Kim, D. F. Bocian, D. Holten, J. S. Lindsey, *J. Mater. Chem.* **2000**, *10*, 283; f) Z. Zhao, T. Nyokong, M. D. Maree, *Dalton Trans.* **2005**, 3732; g) Z. Zhao, C.-T. Poon, W.-K. Wong, W.-Y. Wong, H.-L. Tam, K.-W. Cheah, T. Xie, D. Wang, *Eur. J. Inorg. Chem.* **2008**, 119, and references cited therein.
- [16] a) K. Kameyama, A. Satake, Y. Kobuke, *Tetrahedron Lett.* **2004**, *45*, 7617; b) F. Ito, Y. Ishibashi, S. R. Khan, H. Miyasaka, K. Kameyama, M. Morisue, A. Satake, K. Ogawa, Y. Kobuke, *J. Phys. Chem. A* **2006**, *110*, 12734.
- [17] a) M. Shimomura, S. Aiba, S. Oguma, M. Oguchi, M. Matsute, H. Shimada, R. Kajiwara, H. Emori, K. Yoshiwara, K. Okuyama, T. Miyashita, A. Watanabe, M. Matsuda, *Supramol. Sci.* **1994**, *1*, 33; b) E. H. A. Beckers, S. C. J. Meskers, A. P. H. J. Schenning, Z. Chen, F. Würthner, P. Marsal, D. Beljonne, J. Cornil, R. A. J. Janssen, *J. Am. Chem. Soc.* **2006**, *128*, 649.
- [18] a) C. Kirmaier, D. Holten, E. J. Bylina, D. C. Youvan, *Proc. Natl. Acad. Sci. USA* **1988**, *85*, 7562; b) L. M. McDowell, C. Kirmaier, D. Holten, *J. Phys. Chem.* **1991**, *95*, 3379; c) E. J. P. Lathrop, R. A. Friesner, *J. Phys. Chem.* **1994**, *98*, 3056; d) L. L. Laporte, V. Palaniappan, D. G. Davis, C. Kirmaier, C. C. Schenck, D. Holten, D. F. Bocian, *J. Phys. Chem.* **1996**, *100*, 17696.
- [19] a) A. de la Escosura, M. V. Martínez-Díaz, P. Thordarson, A. E. Rowan, R. J. M. Nolte, T. Torres, *J. Am. Chem. Soc.* **2003**, *125*, 12300; b) X. Li, L. E. Sinks, B. Rybtchinski, M. R. Wasielewski, *J. Am. Chem. Soc.* **2004**, *126*, 10810; c) D. M. Guldi, A. Gouloumis, P. Vázquez, T. Torres, V. Georgakilas, M. Prato, *J. Am. Chem. Soc.* **2005**, *127*, 5811.
- [20] a) V. S.-Y. Lin, S. G. DiMaggio, M. J. Therien, *Science* **1994**, *264*, 1105; b) H. L. Anderson, *Inorg. Chem.* **1994**, *33*, 972; c) A. Tsuda, A. Osuka, *Science* **2001**, *293*, 79.
- [21] a) E. M. Maya, P. Vázquez, T. Torres, *Chem. Eur. J.* **1999**, *5*, 2004; b) E. M. Maya, P. Vázquez, T. Torres, L. Gobbi, F. Diederich, S. Pyo, L. Echegoyen, *J. Org. Chem.* **2000**, *65*, 823.
- [22] a) M. A. Senge, M. Fazekas, E. G. A. Notaras, W. J. Blau, M. Zawadzka, O. B. Locos, E. M. Ni Mhuircheartaigh, *Adv. Mater.* **2007**, *19*, 2737; b) M. Drobizhev, Y. Stepanenko, Y. Dzenis, A. Karotki, A. Rebane, P. N. Taylor, H. L. Anderson, *J. Am. Chem. Soc.* **2004**, *126*, 15352; c) T. K. Ahn, K. S. Kim, D. Y. Kim, S. B. Noh, N. Aratani, C. Ikeda, A. Osuka, D. Kim, *J. Am. Chem. Soc.* **2006**, *128*, 1700.
- [23] O. Shoji, S. Okada, A. Satake, Y. Kobuke, *J. Am. Chem. Soc.* **2005**, *127*, 2201.
- [24] Porphyrin/phthalocyanine stacks: a) J. F. Lipskier, T. H. Tran-Thi, *Inorg. Chem.* **1993**, *32*, 722; b) T. H. Tran-Thi, *Coord. Chem. Rev.* **1997**, *160*, 53; c) T. H. Tran-Thi, S. Gaspard, *Chem. Phys. Lett.* **1988**, *148*, 327; d) A. V. Gusev, M. A. J. Rodgers, *J. Phys. Chem. A* **2002**, *106*, 1985; e) A. V. Gusev, E. O. Danilov, M. A. J. Rodgers, *J. Phys. Chem. A* **2002**, *106*, 1993.
- [25] N. Kobayashi, H. Ogata, N. Nonaka, E. A. Luk'yanets, *Chem. Eur. J.* **2003**, *9*, 5123.
- [26] M. Morisue, K. Kameyama, Y. Kobuke, unpublished results.
- [27] A. de la Escosura, M. V. Martínez-Díaz, D. M. Guldi, T. Torres, *J. Am. Chem. Soc.* **2006**, *128*, 4112.
- [28] A. Ohashi, A. Satake, Y. Kobuke, *Bull. Chem. Soc. Jpn.* **2004**, *77*, 365.

Received: December 10, 2007  
Published online: April 9, 2008